Scientific paper

Structural Study of Simple Organic Acids by Small-Angle X-Ray Scattering and Monte Carlo Simulations

Andrej Lajovic, Matija Tomšič and Andrej Jamnik*

University of Ljubljana, Faculty of Chemistry and Chemical Technology, Aškerčeva 5, SI-1001 Ljubljana, Slovenia

** Corresponding author: E-mail: andrej.jamnik@fkkt.uni-lj.si*

Received: 26-01-2012

Dedicated to Prof. Dr. Gorazd Vesnaver on the occasion of his 70th birthday

Abstract

This study represents an extension of our previous research on the structural properties of simple organic liquids to the systems of organic acids. A set of simple acids from ethanoic to octanoic was modelled with the TraPPE-UA force field and configurational bias Monte Carlo (CBMC) simulations were used to obtain a number of configurations of each system. These data were subsequently used as a basis for the calculation of X-ray scattering intensities, partial radial distribution functions and statistical analysis of molecular aggregation in liquid organic acids. The comparison of simulated X-ray scattering curves with the results of SAXS measurements has shown the agreement to be overall somewhat poorer than in our previous studies on alcohols and aldehydes, although it did improve with increasing molecular length. Hydrogen bonds between the hydroxylhydrogen atom and the carbonyl oxygen have been found to have a profound effect on the structure of the liquid acids. However, the model-based results showed that the formation of intermolecular hydrogen bonds involving the hydroxyl oxygen was disproportionately scarce in these systems. Statistical evaluation of the model configurations has shown that only about 4% of acid molecules form such a type of hydrogen bonds, in contrast to 68% of molecules that form the hydrogen bond with the carbonyl oxygen. This suggests that the force field might be underestimating the hydrogen bonding via hydroxyl oxygen. The statistical analysis has also shown that the simulated molecules preferred to assemble into small molecular aggregates, particularly into double-bonded molecule pairs.

Keywords: Small-angle X-ray scattering, TraPPE-UA, CBMC.

1. Introduction

The motivation for our interest in structural investigations of simple organic liquids originates in our previous structural studies of special microemulsions based on simple organic alcohols that had been tested as media for biocatalytic synthesis of aldehydes.[1–5] In these studies it was realized that molecules in pure simple alcohols, as well as in pure simple aldehydes, structurally organize themselves due to their partially amphiphilic character. Such molecular organization seemed to govern the structure of alcohol-rich microemulsions and was therefore assessed to be worthwhile exploring further.

During the last few years we have in this manner developed a special approach for the calculation of the small-angle scattering intensities from the Monte Carlo simulation results, which were then compared with the experimental data.[6–8] For example, we have conducted numerous studies on the structure of pure simple alcohols[6,7,9–11] and aldehydes.[12] Especially simple organic alcohols are commonly used as co-surfactants in various surfactant systems. Detailed information on the molecular organization in organic liquids is therefore of very broad interest and general relevance. Our previous studies showed, among others, that intermolecular hydrogen bonding considerably affects the structure of such pure liquids, as was demonstrated by the qualitative difference in the intermolecular bonding of alcohols (containing the hydroxyl (–OH) group) and aldehydes (containing the carbonyl (–CO) group as a part of aldehyde (–CHO) group). Exploring the structural situation in a liquid containing the carboxyl (–COOH) group, which combines the properties of both mentioned functional groups, seems to be the next logical step forward.

In the present study we therefore aim to obtain detailed structural information on simple carboxylic acids from ethanoic to octanoic acid. For this purpose, the acid

molecules were modelled utilizing the transferable potential for phase equilibria – united atom (TraPPE-UA) force field[13] and configurational bias Monte Carlo (CBMC) simulations were performed.[14,15] The resulting MC configurations were then used in the calculations of the X-ray scattering intensities, as described into more detail later in the text. The obtained theoretical results were then discussed and compared to the experimental small-angle X-ray scattering (SAXS) data in the regime of scattering vector $0.3 < q < 25$ nm^{-1}, where q represents the length of the scattering vector $q = 4\pi/\lambda \cdot \sin(\vartheta/2)$, with λ being the wavelength of the X-rays and ϑ the scattering angle.

2. Experimental and Methods

2. 1. Materials

Ethanoic, propanoic and octanoic acid were purchased from Sigma-Aldrich; butanoic, pentanoic and hexanoic acid from Aldrich and heptanoic acid from Sigma (purities: ethanoic ≥ 99.99 %, propanoic ≥ 99.5 %, butanoic ≥ 99 %, pentanoic ≥ 99 %, hexanoic ≥ 99 %, heptanoic ≥ 97 %, octanoic ≥ 99 %). Based on our previous experience and tests, even up to 3 % of impurities do not cause a noticeable degrading effect on the measurements. All purchased compounds have been therefore used without further purification.

2. 2. Small-Angle X-Ray Scattering Measurements

Small-angle X-Ray scattering spectra were measured with a "SAXSess" evacuated high performance SAXS instrument (Anton Paar KG, Graz, Austria), which was attached to a conventional X-ray generator (Philips, Netherlands) equipped with a sealed X-ray tube (CuK_α X-rays with a wavelength $\lambda = 0.154$ nm) operating at 40 kV and 50 mA. The samples were measured at 25 °C in a standard quartz capillary for the SAXSess camera with an outer diameter of 1 mm and wall thickness of 10 μm. A Fuji BAS 1800 2D-imaging plate detection system with a spatial resolution of 50 × 50 μm per pixel at a sample-to-detector distance of 265 mm was used. After 30-minute measurements the scattering data were read off the imaging plate, then corrected for the absorption of X-rays in the sample and transformed to the q scale (program SAXSQuant; Anton Paar KG, Graz, Austria). The scattering intensities were further corrected for the empty capillary scattering and put to the absolute scale using water as a secondary standard[16] (program PDH; PCG software, Institute of Chemistry, Graz, Austria). Due to the line collimation of the X-ray beam used in the measurement, the scattering curves were still experimentally smeared at this point. To recover the true intensities, we employed a technique described by Glatter in the article on indirect Fourier transformation of the scattering data.[17] A set of base functions covering the q-range in question was constructed and the functions were subsequently numerically smeared utilizing the width- and length-profiles of the X-ray beam. A linear least-squares fitting procedure was performed to obtain a set of coefficients that provided the best fit of the smeared base functions to the experimental scattering curve. The desmeared intensities were finally recovered by summing the set of original base functions weighted with the coefficients obtained in the previous step.The fact that the length-profile of the primary beam was rather narrow in comparison to the broad q regime being covered by SAXS measurements justified such an approach for desmearing of the experimental SAXS curves.

2. 3. Model and Simulation Details

The TraPPE-UA (Transferable Potential for Phase Equilibria – United Atom) force field[18–20] was used to model the organic acids from ethanoic to octanoic. Due to the united-atom approach used by this force field, all hydrogen atoms–except the hydroxyl hydrogen–were treated implicitly as a part of their respective CH_X groups. The model molecules thus consisted of a hydroxyl hydrogen atom, a hydroxyl oxygen atom (denoted from here on as O[OH]), a carbonyl oxygen atom (denoted as O[CO]), a carbonyl carbon atom, and a variable number of CH_2 pseudo-atoms, followed by a terminal methyl pseudo-atom.

The configurational bias Monte Carlo (CBMC)[14] simulation technique was used to generate a number of independent configurations of these acids in the NVT ensemble. The numbers of molecules and the side lengths of the simulation boxes were as follows: ethanoic acid (500, 36.22 Å), propanoic acid (500, 39.58 Å), butanoic acid (500, 42.40 Å), pentanoic acid (500, 45.01 Å), hexanoic acid (500, 47.15 Å), heptanoic acid (500, 49.01 Å) and octanoic acid (500, 50.86 Å).

A spherical truncation at 14 Å was used for the Lennard-Jones part of the potential, and analytical corrections for the tail were employed. The Ewald summation was used for the long-range Coulombic interactions with the summation range in reciprocal space $\kappa_{max} = 5$ and the Ewald convergence parameter $\kappa\alpha = 5.6$. Three types of Monte Carlo steps were used (relative probabilities of their usage are given in brackets): configurational bias partial molecule regrowth (40%), center-of-mass molecule translation (30%), and rotation about center-of-mass (30%). Maximum displacements for the latter two were automatically adjusted during equilibration to yield 50% acceptance ratios. Each system was equilibrated for 30,000 cycles (one cycle consisted of the same number of Monte Carlo steps as there were molecules in the system), followed by a production run of 30,000 cycles. During this run, a snapshot of particle coordinates was saved every 300 cycles and the resulting 100 configurations were later used to calculate the scattering intensities, partial radial distribution functions and for the statistical analysis.

All simulations were performed with the MCCCS Towhee Monte Carlo simulation code, version 6.2.12.[21]

2. 4. Calculation of the Scattering Intensities

X-ray scattering intensities were calculated from the simulation results via the complemented system approach.[8] This recently developed method employs a direct application of the Debye equation[22] to the particle positions, combined with an analytical complementary term that accounts for the finiteness of the simulation box. As a consequence, no intermediate results and/or binning are necessary and the resulting absolute intensities correspond as closely as possible to the structure of the simulated systems.

The following equation was used to calculate the differential scattering cross-section per unit volume, $d\Sigma/d\Omega$ (sometimes also called the *absolute intensity*):

$$d\Sigma/d\Omega = \frac{r_e^2}{V}\left\langle \sum_{j=1}^{N}\sum_{k=1}^{N} f_j(q)\, f_k(q)\, \frac{\sin(qR_{jk})}{qR_{jk}}\, H(r_c - R_{jk}) \right\rangle + \\ + \left(\sum_{A=1}^{T} b_A(q)\, \rho_A \right)^2 \left[(2\pi)^3\, \delta(q) - \frac{4\pi}{q^3}\left[\sin(qr_c) - qr_c\cos(qr_c)\right] \right] \quad (1)$$

The first term in the right-hand side of the above equation is the Debye equation: V is the volume of the simulated system, r_e is the classical electron radius (2.81794×10^{-15} m), N is the number of particles in the system, indices j and k denote the j-th and the k-th particle, $f_j(q)$ and $f_k(q)$ are their respective atomic form factors, R_{jk} the distance between them, r_c the cut-off distance ($r_c = L/2$ with L being the side length of the simulation box) and $H(r)$ is the Heaviside step function. For true atoms, the atomic form factors were calculated using an analytical expression and tabulated coefficients,[23] whereas for the united atoms, the form factors were approximated with the help of the Debye equation.[7] The angled brackets denote the canonical average which was performed in this case by averaging the results over all the configurations saved during the simulation. The second term represents the average surroundings of each particle: T is the number of particle types in the system, ρ_A is the number density of particles of the A-th type and $\delta(q)$ is the Dirac delta function.

The lower bound for the q-scale in each calculation was determined from the side length of the simulation box: $q_{min} = 2\pi/(L/2)$ where q_{min} is the minimum q used in the calculation.

3. Results and Discussion

3. 1. Experimental and Theoretical X-Ray Scattering Curves

Both the experimental scattering intensities and the scattering curves calculated from the CBMC simulations

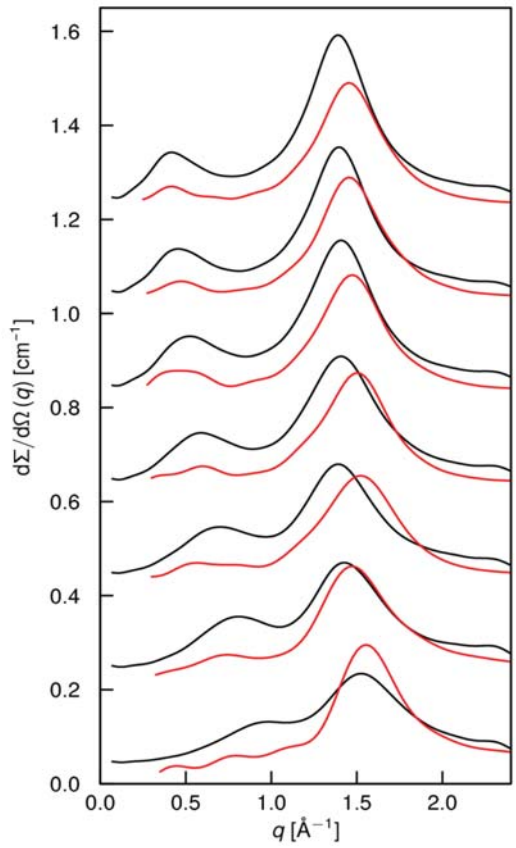

Figure 1. SAXS curves of organic acids from ethanoic (bottom) to octanoic (top). Experimental results are drawn in black colour and the scattering curves calculated from the simulation data in red. The curves from propanoic acid on are shifted upwards by multiples of 0.2 cm^{-1} for the sake of clarity.

are shown in Figure 1. The experimental scattering curves feature two peaks: the higher peak resides at the value of the scattering vector $q \approx 1.4$ Å^{-1} and is relatively independent of the chain length, whereas the lower peak is situated at about $q \approx 1.0$ Å^{-1} for ethanoic acid and progresses towards lower values as the molecule size increases (for octanoic acid, the peak is found at $q \approx 0.4$ Å^{-1}). To estimate the correlation lengths that give rise to these two peaks, the characteristic real-space distances r_o can be calculated using the relation $r_o = 2\pi/q$. The reciprocal distance of $q \approx 1.4$ Å^{-1} (i.e., the position of the higher peak) thus translates into the real-space distance of approximately 4.5 Å. Such a distance is usually interpreted as an effective average distance between the molecules and the emergence of a similar peak in many other systems (alcohols, aldehydes, ketones) confirms that this is indeed the case. As shown in Figure 2, the correlation lengths corresponding to the smaller (inner) peak lie in the range from about 6 Å for ethanoic to approximately 15 Å for octanoic acid and their relationship to the number of carbon atoms in the molecule is found to be almost perfectly linear. In order to investigate a possible relation between these correlation lengths and the true lengths of the molecules, a set of geometry optimiza-

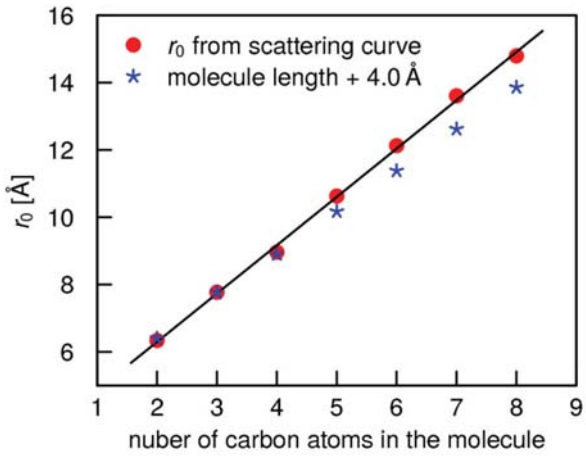

Figure 2. Correlation lengths calculated from the position of the inner peak on the scattering curve (full circles) and molecule lengths (distances from CH_3 to O[OH]) calculated *in vacuo* by the semiempiric method PM3 (stars). A constant offset of 4.0 Å was added to the molecule lengths to facilitate the comparison; the constant was selected so as to make the points for ethanoic acid coincide.

tions were performed *in vacuo*, utilising the semiempiric method PM3. The resulting distances between the CH_3 pseudo atom and the hydroxyl oxygen atom were measured and again plotted versus the number of carbon atoms in the molecule (see Figure 2). Interestingly, this relation also turned out to be linear, with the slope slightly smaller, but still very similar as in the case of the relationship between the correlation lengths and the number of carbon atoms. This similarity presents strong evidence that the characteristic distance of the correlation from which the inner peak arises corresponds to the distance between some significant points on the molecules: as the molecule size increases, so does the separation of such points in the system. Given that the functional groups are the only points of strong scattering contrast in the molecules, we conclude that the correlations between them are the most probable cause for the emergence of the inner peak.

The agreement between the experimental and simulated scattering curves is not as good as had been expected from our previous results on alcohols[6,7] and aldehydes.[12] Especially in the case of shorter molecules (propanoic to butanoic acid), the simulation tends to overestimate the outer (larger) peak and to underestimate the inner one. Also, the predicted position of the outer peak differs from the experimentally determined value. In fact, the position of the scattering peak is much more indicative in relation to the actual structure than the absolute peak height, because it reflects the characteristic distances, correlation lengths and other structural features in the sample. At a given size of the local structure which gives rise to the scattering peak at a specific position, the height of the peak depends mainly on the scattering contrast of this structure against the surroundings. Disagreement between the experimental and calculated heights of the peak thus stems from an inaccurate value of the scattering contrast used in the theoretical calculations. However, a somewhat poorer accuracy in matching the model and actual scattering contrasts does not have a significant effect on the positions of the peaks in the q-scale, from which the main structural characteristics can be deduced.

From pentanoic acid on, the agreement with experiment improves considerably, although the position of the outer peak remains shifted. This suggests that the cause of the poor agreement might lie in the force field's treatment of the interactions between the functional groups, since their influence on the structure of the liquid is greatest when the molecules are short. As the length of the molecules increases, the interactions between the nonpolar carbon chains gain significance and the influence of the interactions between the functional groups diminishes.

Although the modest agreement between the numerical and experimental results restrains us from drawing a firm parallel between the true and simulated systems, the results are anyway worth examining, if only with the intent of identifying the possible causes of the force field's poor performance in predicting the structure of organic acids on the molecular level.

3. 2. Partial Radial Distribution Functions

Intermolecular partial radial distribution functions (PRDFs) were calculated from the configurations saved during the simulation. Each type of (pseudo-) atom was considered to be its own entity. To keep the number of displayed partial radial distribution functions manageable and to concentrate our inquiry on the set of the intermolecular interactions that we deem most important, we will constrain our presentation to the partial radial distribution functions involving either the hydroxyl hydrogen atom or the carbonyl oxygen atom in the propanoic acid molecule as depicted in Figure 3 and 4.

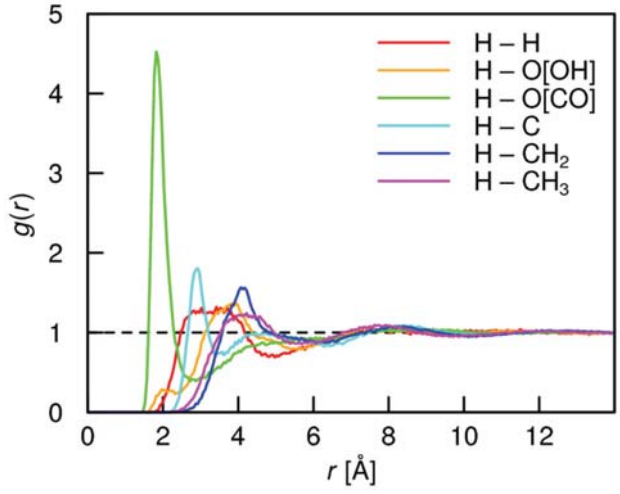

Figure 3. Partial radial distribution functions of the hydrogen atom in the propanoic acid molecule.

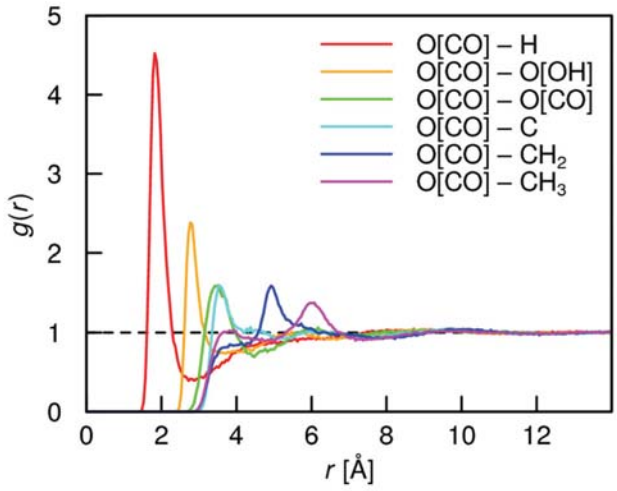

Figure 4. Partial radial distribution functions of the carbonyl oxygen atom in the propanoic acid molecule.

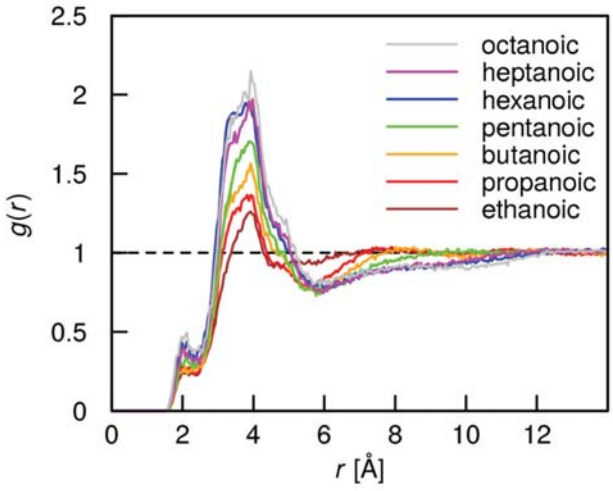

Figure 5. Partial radial distribution functions H-O[OH] for organic acids from ethanoic to octanoic

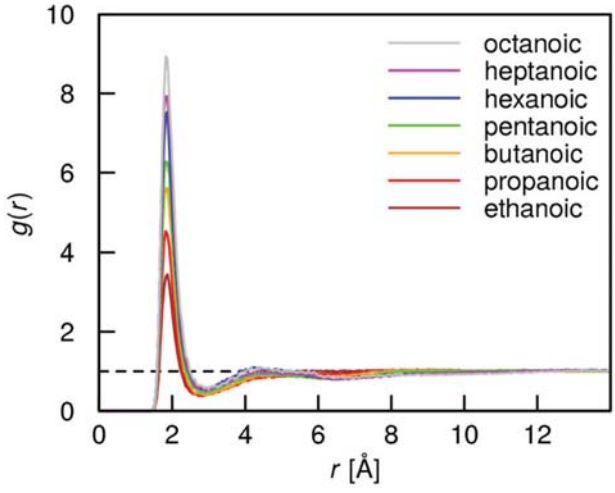

Figure 6. Partial radial distribution functions H-O[CO] for organic acids from ethanoic to octanoic.

The most prominent feature seen on both figures is the strong first peak on the PRDF of the pair H-O[CO]. Located at an oxygen-to-hydrogen distance of 1.8 Å, it is a typical sign of hydrogen bonding. Observing the positions of the peaks in Figure 4, one can see how the hydrogen bond dictates the mutual orientation of the molecules: the hydrogen atom makes the closest approach to the O[CO] atom, after which the rest of the atoms follow in the same order as they appear in the molecule: O[OH], then O[CO] and C (at approximately the same distance), followed by CH_2 and CH_3. The whole molecule thus orients in such a way as to enable the formation of the hydrogen bond. The effect of such a strong intermolecular correlation is also reflected in the fact that the PRDFs do not return to their average value of one until the distance of approximately 10 Å.

Figure 3 also reveals another, rather peculiar, fact. Since the carboxyl functional group contains two oxygen atoms capable of forming hydrogen bonds,[24] one would expect the shapes of the PRDFs H-O[CO] and H-O[OH] to be similar (very high first peak at a relatively short distance). However, the latter shows almost no signs of hydrogen bonding and its maximum value is even exceeded by a few other PRDFs. At $r \approx 2$ Å, a small unexpressed peak can be observed, which indicates that at least a few hydrogen bonds may have been established via this atom. Nevertheless, the peak value is markedly less than one, whereas it would be ordinarily expected to greatly exceed one. This discordance leads us to believe that the force field had significantly underestimated one of the main types of correlations in the system, which might well be the reason for the poor agreement between the experimental and numerical results.

To check whether the rest of the simulated systems also suffer from the same deficiency, a set of H-O[OH] PRDFs for acids from ethanoic to octanoic is compared in Figure 5 and a set of H-O[CO] PRDFs for the same systems in Figure 6. It is evident, despite the differing absolute values of the functions within each set, that their shapes do not alter much with the changing molecular length. Most importantly, the proportion of the small peak at $r \approx 2$ Å on the PRDF for the pair H-O[OH] to the large peak on the PRDF for the pair H-O[CO] also does not change significantly. This means that the hydrogen bonds involving the carbonyl oxygen atom remain dominant in relation to those involving the hydroxyl oxygen. Underestimation of the latter type of hydrogen bonding is therefore a problem of the quality of the model, as it is observed for all of the investigated molecules regardless of their chain length. This also confirms that the most probable cause for the improvement in the agreement between the experimental and numerical results of longer molecules is that, as the molecule length increases, the interactions between the functional groups play an increasingly smaller role,

while the interactions between the nonpolar chains begin to control the overall structure of the liquid.

3. 3. Molecular Aggregation

Partial radial distribution function H-O[CO] presented in Figure 4 can be conveniently used to define an association criterion, i.e., to define the condition under which two molecules are considered bonded. Since the first peak of the function represents the hydrogen-bonded pairs, a suitable condition would be that the H-O[CO] distance between the molecules fall within it. This definition brings with it an ambiguity about what exactly is considered the maximum distance that still falls within the peak. The distance where the peak attains its maximum value is clearly insufficient for that purpose, since almost one half of the pairs (those with distances even slightly larger than this) would be left out. Another two possibilities would be either the point where the function first returns to the value of one or the distance of the first minimum after the peak. In the case of organic acids, both are unambiguous, but in other systems, they are often not, which has led us to another definition that can be used universally: the maximum pair distance between the atoms of the associated molecules is the distance of the first point of inflection after the first maximum on the partial radial distribution function.

For propanoic acid, the maximum pair distance H-O[CO] was determined to be 1.98 Å; this is a typical result for this set of acids, since the values for other investigated compounds all fell in the range from 1.97 Å to 2.02 Å. The results of the statistical analysis of the saved configurations are shown in Figure 7. In principle, the pairs with H-O[OH] hydrogen bonds should also have been included in the analysis, but their number is so low (only about 4% of the molecules form this type of bond) that the results would not be altered appreciably.

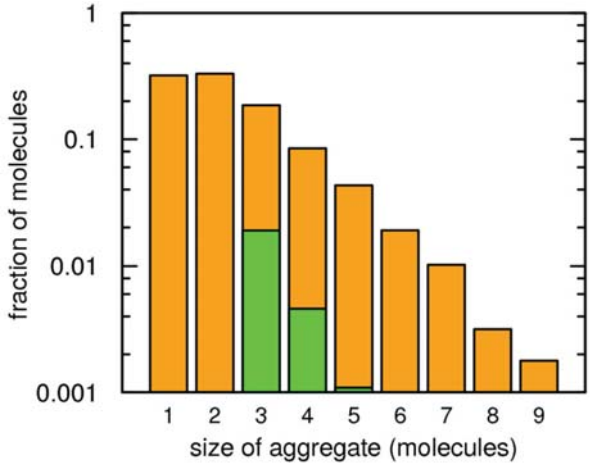

Figure 7. Histograms of the fraction of propanoic acid molecules versus the aggregate size (orange) and the fraction of propanoic acid molecules in aggregates that contain at least one closed cycle (green).

As we can see from Figure 7, only about one third of the molecules are not involved in hydrogen bonding; the rest of them are distributed within aggregates of various sizes, with notable bias towards the smaller ones. Of these, molecular pairs tend to be the most frequent-in fact, the majority of the molecules can be found in such a configuration. The reason for their favourability is their capability of establishing two hydrogen bonds within a single pair and thus forming a doubly connected pair. However, such pairs are relatively "closed" with respect to the formation of additional hydrogen bonds, with consequently lower frequencies of aggregates comprising three or more molecules. From that point on, the distribution assumes an exponential shape (which shows as a linear decrease on the logarithmic scale in Figure 7).

The histogram also shows the fractions of molecules found in aggregates that contain at least one cyclic part. Such structures are relatively scarce: only aggregates with three and four members are present in significant amounts. Of the latter, virtually all are the true cyclic structures (as opposed to a combination of cyclic and linear parts). Typical examples of a three-membered and four-membered cyclic aggregate are shown in Figure 8 and 9. Obviously, the structure of the three-membered cycle is much simpler, as the shape of the molecules allows it to be nearly planar. The four-membered cycle, on the other hand, cannot be formed in a single plane and therefore needs to assume a more complicated configuration. This difference also accounts for the prevalence of the three-membered cycles over four-membered ones.

4. Conclusions

In this study, we have extended our research on the structural properties of simple organic liquids to the systems of organic acids. Surprisingly, the agreement bet-

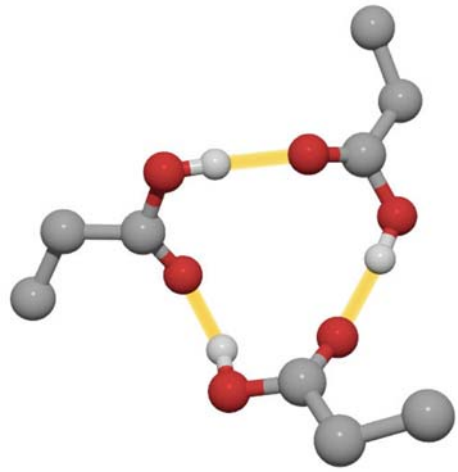

Figure 8. A typical cyclic aggregate formed by three molecules of propanoic acid. Hydrogen bonds are drawn in orange colour.

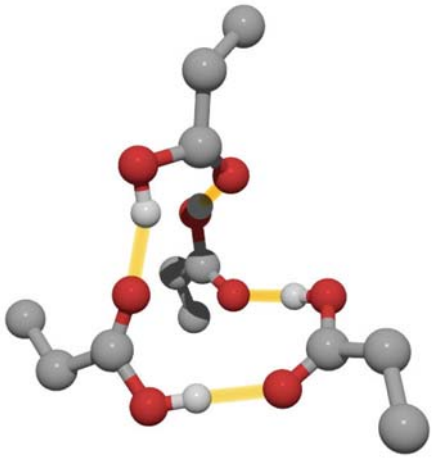

Figure 9. A typical cyclic aggregate formed by four molecules of propanoic acid. Hydrogen bonds are drawn in orange colour.

ween the experimental and simulated X-ray scattering curves was somewhat poorer than in the case of alcohols[6] and aldehydes,[12] particularly in shorter molecules. Judging from the partial radial distribution functions obtained from the saved Monte Carlo configurations, we have good reason to believe that the discrepancy originates in the force field's treatment of the hydrogen bonds involving the hydroxyl oxygen atom. While the partial radial distribution function for hydroxyl hydrogen and carbonyl oxygen shows a strong peak that resembles the one found in alcohols, there is no such feature seen on the partial radial distribution function of hydroxyl hydrogen and hydroxyl oxygen. Instead, only a small, barely recognizable peak is present. By the means of a statistical analysis, it was revealed that only about 4% of the molecules form such a bond-in contrast to the 68% of molecules that are hydrogen-bonded via the carbonyl oxygen. Although the strength and frequency of hydrogen bonds can vary between the various pairs of atoms capable of forming it, we feel that this difference is, nevertheless, too large.

For simulations of phase equilibria of organic acids, the TraPPE-UA force field seems to remain a reliable choice,[20,25] since its primary aim is (as the name suggests) to provide the best possible predictions in that respect. For simulations wanting to reproduce the correct structure of simple organic acids in the bulk, however, we deem that other (possibly all-atom) force fields should be given a try.

5. Acknowledgements

We are thankful to prof. Otto Glatter from the Institute of Chemistry, University of Graz, for the warm welcome in his lab, and to Günther Scherf for the assistance with the SAXS experiments. We also acknowledge financial support from the Slovenian Research Agency through the Physical Chemistry Research Programme 0103-0201 and from the Federal Ministry for Education, Science, and Culture of Austria (BI-AT/09-10-022).

6. References

1. A. Meziani, D. Touraud, A. Zradba, S. Pulvin, I. Pezron, M. Clausse, W. Kunz, *J. Phys. Chem. B* **1997**, *101*, 3620–3625.
2. H. Preu, A. Zradba, S. Rast, W. Kunz, E. H. Hardy, M. D. Zeidler, *Phys. Chem. Chem. Phys.* **1999**, *1*, 3321–3329.
3. C. Schirmer, Y. Liu, D. Touraud, A. Meziani, S. Pulvin, W. Kunz, *J. Phys. Chem. B* **2002**, *106*, 7414–7421.
4. M. Tomšič, M. Bešter-Rogač, A. Jamnik, W. Kunz, D. Touraud, A. Bergmann, O. Glatter, *J. Phys. Chem. B* **2004**, *108*, 7021–7032.
5. M. Tomšič, M. Bešter-Rogač, A. Jamnik, W. Kunz, D. Touraud, A. Bergmann, O. Glatter, *J. Colloid Interf. Sci.* **2006**, *294*, 194–211.
6. M. Tomšič, A. Jamnik, G. Fritz-Popovski, O. Glatter, L. Vlček, *J. Phys. Chem. B* **2007**, *111*, 1738–1751.
7. M. Tomšič, G. Fritz-Popovski, L. Vlček, A. Jamnik, *Acta. Chim. Slov.* **2007**, *54*, 484–491.
8. A. Lajovic, M. Tomšič, A. Jamnik, *J. Chem. Phys.* **2010**, *133*, 174123.
9. M. Tomšič, A. Jamnik, in: M. Fanun (Ed.): Microemulsions: Properties and Applications, CRC Press, Boca Raton, **2009**, pp. 143–183.
10. A. Vrhovšek, O. Gereben, S. Pothoczki, M. Tomšič, A. Jamnik, L. Pusztai, *J. Phys.: Condens. Matter* **2010**, *22*, 404214.
11. A. Vrhovšek, O. Gereben, A. Jamnik, L. Pusztai, *J. Phys. Chem. B* **2011**, *115,* 13473-13488.
12. A. Lajovic, M. Tomšič, G. Fritz-Popovski, L. Vlček, A. Jamnik, *J. Phys. Chem. B* **2009**, *113*, 9429–9435
13. J. M. Stubbs, J. J. Potoff, J. I. Siepmann, *J. Phys. Chem. B* **2004**, *108*, 17596–17605
14. J. I. Siepmann, D. Frenkel, *Mol. Phys.* **1992**, *75*, 59–70.
15. T. J. Vlugt, M. G. Martin, B. Smit, J. I. Siepmann, R. Krishna, *Mol. Phys.* **1998**, *94*, 727–733.
16. D. Orthaber, A. Bergmann, O. Glatter, *J. Appl. Crystallogr.* **2000**, *33*, 218–225.
17. O. Glatter, *J. Appl. Crystallogr.* **1977**, *10*, 415–421.
18. M. G. Martin, J. I. Siepmann, *J. Phys. Chem. B* **1998**, *102*, 2569–2577.
19. B. Chen, J. J. Potoff, J. I. Siepmann, *J. Phys. Chem. B* **2001**, *105*, 3093–3104.
20. G. Kamath, F. Cao, J. J. Potoff, *J. Phys. Chem. B* **2004**, *108*, 14130–14136
21. MCCCS Towhee. http://towhee.sourceforge.net
22. P. Debye, *Ann. Phys.***1915**, *315*, 809–823.
23. D. Waasmaier, A. Kirfel, *Acta Crystallographica Section A* **1995**, *51*, 416–431.
24. W. Xu, J. Yang, *J. Phys. Chem. A* **2010**, *114*, 5377–5388.
25. S. Clifford, K. Bolton, D. Ramjugernath, *J. Phys. Chem. B* **2006**, *110*, 21938–21943.

Povzetek

V pričujočem delu smo teorijske in eksperimentalne raziskave strukture nekaterih preprostih organskih tekočin, ki smo ji opravili v prejšnjih raziskavah, razširili še na preproste organske kisline. Organske kisline od etanojske do oktanojske smo modelirali na osnovi polja sil TraPPE-UA in izvedli poseben tip konfiguracijsko usmerjanih simulacij Monte Carlo (MC) (angl. »*configurational bias Monte Carlo simulations*«). Shranjene MC-konfiguracije smo uporabili za izračun intenzitet ozkokotnega rentgenskega sipanja in parskih porazdelitvenih funkcij ter za statistično analizo pojavljanja molekulskih gruč (agregatov) v teh sistemih. Izračunane sipalne funkcije smo nato primerjali z eksperimentalnimi rezultati rentgenskega sipanja. Ujemanje teorijskih napovedi sipanja z eksperimentalnimi rezultati je bilo nekoliko slabše kot v primeru alkoholov in aldehidov, ki smo jih obravnavali v prejšnjih raziskavah, se je pa nekoliko izboljševalo z daljšanjem ogljikove verige v molekulah kislin. Ugotovili smo, da imajo vodikove vezi med hidroksilnimi vodikovimi atomi in atomi kisika karbonilnih skupin pomemben vpliv na strukturo tekočih organskih kislin, medtem ko je vloga vodikovih vezi, ki vključujejo atome kisika hidroksilnih skupin, neprimerno manjša. Statistična obdelava teorijskih rezultatov je namreč pokazala, da se s tovrstnimi vodikovimi vezmi povezuje le okoli 4 % molekul kislin, medtem ko je okoli 68 % molekul kislin povezanih z vodikovimi vezmi preko atomov kisika karbonilnih skupin. Dejstvo, da je med izračunanimi in eksperimentalnimi rezultati rentgenskega sipanja nekaj odstopanja, nakazuje, da so vodikove vezi preko kisikovih atomov hidroksilnih skupin v uporabljenem modelu verjetno podcenjene. Statistična analiza modelnih rezultatov je pokazala tudi, da se molekule kislin povezujejo večinoma v manjše molekulske skupke – najpogosteje je najti molekulske pare, v katerih sta kislinski molekuli povezani z dvema vodikovima vezema hkrati.